ELSEVIER

International Journal of Minerals, Metallurgy and Materials
Volume 16, Number 6, December 2009, Page 654

Materials

Intergranular corrosion behavior of high nitrogen austenitic stainless steel

Hua-bing Li, Zhou-hua Jiang, Zu-rui Zhang, Yang Cao, and Yan Yang

School of Materials and Metallurgy, Northeastern University, Shenyang 110004, China
(Received 2008-12-15)

Abstract: The intergranular corrosion (IGC) behavior of high nitrogen austenitic stainless steel (HNSS) sensitization treated at 650-950°C was investigated by the double loop electrochemical potentiodynamic reactivation (DL-EPR) method. The effects of the electrolytes, scan rate, sensitizing temperature on the susceptibility to IGC of HNSS were examined. The results show that the addition of NaCl is an effective way to improve the formation of the cracking of a passive film in chromium-depleted zones during the reactivation scan. Decreasing the scan rate exhibits an obvious effect on the breakdown of the passive film. A solution with 2 mol/L H_2SO_4+1 mol/L NaCl+0.01 mol/L KSCN is suitable to check the susceptibility to IGC of HNSS at a sensitizing temperature of 650-950°C at a suitable scan rate of 1.667 mV/s. Chromium depletion of HNSS is attributed to the precipitation of Cr_2N which results in the susceptibility to IGC. The synergistic effect of Mo and N is suggested to play an important role in stabilizing the passive film to prevent the attack of IGC.

Key words: intergranular corrosion; high nitrogen austenitic stainless steel; sensitization; passive film; chromium depletion

[*This work was financially supported by the National Natural Science Foundation of China (No.50534010) and Baosteel Group Corporation.*]

1. Introduction

Intergranular corrosion (IGC) is one of the major local corrosion problems faced by austenitic stainless steel used in various industries including nuclear, thermal power, chemical, petrochemical, pulp, oil and refineries. IGC refers to the preferential corrosion attack along the grain boundaries in certain corrosive environments which results in the loss of engineering properties [1]. It is widely accepted that the IGC attack is caused in the chromium depletion area along the boundaries and adjacent regions due to chromium carbide [2-5] and other intermetallic phases [6-7]. To characterize the grain boundary susceptibility against corrosion attack, the electrolytic oxalic acid test and the electrochemical potentiodynamic reactivation (EPR) method have been used. The EPR method including single loop EPR [8-9] and double loop EPR (DL-EPR) [10-12] provides a rapid, quantitative, and nondestructive way to evaluate the susceptibility to IGC, and the DL-EPR method has been widely applied in determining the IGC of stainless steels [13-15]. The IGC investigation by the DL-EPR method on nitrogen alloyed stainless steels, especially on high nitrogen austenitic stainless steel (HNSS) is few [6, 16]. And the sensitivity and the selectivity of the DL-EPR method in the detection of chromium depleted zones seem to depend markedly on the test conditions such as electrolytes, scan rate, and sensitizing temperature [14-15, 17]. So it is very necessary to select suitable experimental conditions for evaluating the susceptibility to IGC of high nitrogen steels with different chromium depleted states.

In the present work, the IGC behavior of HNSS was examined by the DL-EPR method. The research on precipitation behavior of HNSS sensitization treated at 650-950°C was carried out. A suitable electrolyte and scan rate was explored for determining the susceptibility to IGC. The effect of sensitizing temperature on the susceptibility to IGC was investigated, and the mechanism was also discussed.

2. Experimental procedure

The material used in this study was HNSS, and its chemical composition is shown in Table 1. The HNSS

Corresponding author: Zhou-hua Jiang, **E-mail:** jiangzh@smm.neu.edu.cn
Also available online at www.sciencedirect.com

was manufactured by a vacuum induction furnace and an electro-slag remelting furnace under nitrogen atmosphere [18]. The specimens of 10.1 mm×10.1 mm×3 mm were machined from a hot rolled sheet, and then were solution annealed at 1100°C for 1 h followed by water quenching. The sensitization treatments of the specimens were cooled at 650-950°C for 2 h and followed by air cooling. The electrolytic etching with 10wt% oxalic acid solution was used to reveal the microstructure, and the precipitation in the sensitization treatment steels was identified by the transmission electron microscopy (TEM).

Table 1. Chemical composition of HNSS used in present study **wt%**

C	Si	Cr	Mn	Mo	Ni	S	P	Al	O	N	Fe
0.022	0.19	19.84	18.9	2.26	—	0.002	≤0.03	0.02	0.0042	0.88	Bal.

The specimens for corrosion resistance evaluation were mounted in an epoxy resin with an exposed area of 1 cm^2 and polished with SiC paper from 200 grit to 800 grit. The DL-EPR method was used to determine the susceptibility to IGC. All the measurements were carried out using a potentiostat PARSTAT 2273, which was comprised of 3 electrodes. A platinum foil and a saturated calomel electrode (SCE) were used as the counter and reference electrodes, respectively. The two types solutions of H_2SO_4+KSCN and H_2SO_4+NaCl+KSCN were prepared to explore the suitable test solution in present work. The solution was de-aerated with high purity nitrogen gas before testing for half an hour. During the DL-EPR tests, the specimens were polarized anodically first through the active region to passive region, leading to the formation of a passive layer on the whole surface. Then the reactivation scan in the reverse direction was carried out at the same scan rate, leading to the breakdown of the passive film on chromium depleted area. As a result, an anodic loop and a reactivation loop were generated. The different scan rates were employed to investigate the effect of the scan rate on the DL-EPR results. The IGC susceptibility of the steel was evaluated by comparing the ration of the peak reactivation current density I_r and the peak activation current density I_a, the reactivation electric charge Q_r and the activation electric charge Q_a, respectively. Above all experiments, the experimental temperature and the potential scan range were controlled at 30°C and from −500 to 200 mV (*vs*. SCE), respectively.

3. Results and discussion

3.1. Microstructure

Fig. 1 shows the optical micrographs of HNSS sensitization treated at 650-950°C for 2 h followed by air cooling. Cr_2N precipitation is first observed to nucleate along grain boundaries with 0.005vol% by quantitative metallographic analysis as shown in Fig. 1(a). With increasing sensitizing temperature, the amount of Cr_2N precipitation increases so much that the grain boundaries are covered almost as shown in Figs. 1(b) and 1(c). At 800°C, the intergranular precipitation keeps on coarsening and lamellae Cr_2N first precipitates along grain boundaries with a small cellular zone as shown in Fig. 1(d). The cellular zone expands with increasing the sensitization temperature to 850°C, which results in several distinct areas within grains covered with the cellular Cr_2N precipitation as shown in Fig. 1(e). When the temperature increased to 900 and 950°C, Cr_2N precipitation occurred along grain boundaries decreases gradually as shown in Figs. 1(f) and 1(g), respectively.

The σ, χ and M_7C_3 of precipitation phases of 18Cr-18Mn-2Mo-0.9N steel were found by Lee [19] within grains or along cell boundaries after long aging time. The formation of precipitated phases was attributed to the nitrogen depletion for the formation of Cr_2N precipitation in HNSS. But in the present work, there was not enough aging time for the nucleation and growth of σ, χ and M_7C_3. Based on the analyses of selected area diffraction (SAD) patterns, the coarse intergranular precipitation (500-600 nm) and cellular precipitation (200 nm in thickness) are identified as Cr_2N with hexagonal structure during the sensitization treatment as shown in Figs. 2 and 3, respectively. Fig. 4 shows the sensitizing temperature dependence of the volume fraction of Cr_2N precipitation. The volume fraction increases first then reduces with increasing the sensitizing temperature.

3.2. DL-EPR results

(1) Exploring the suitable electrolyte and the scan rate

To obtain the suitable parameters of the DL-EPR method to evaluate quantitatively the susceptibility to IGC, DL-EPR experiments were performed at different experimental conditions as shown in Table 2.

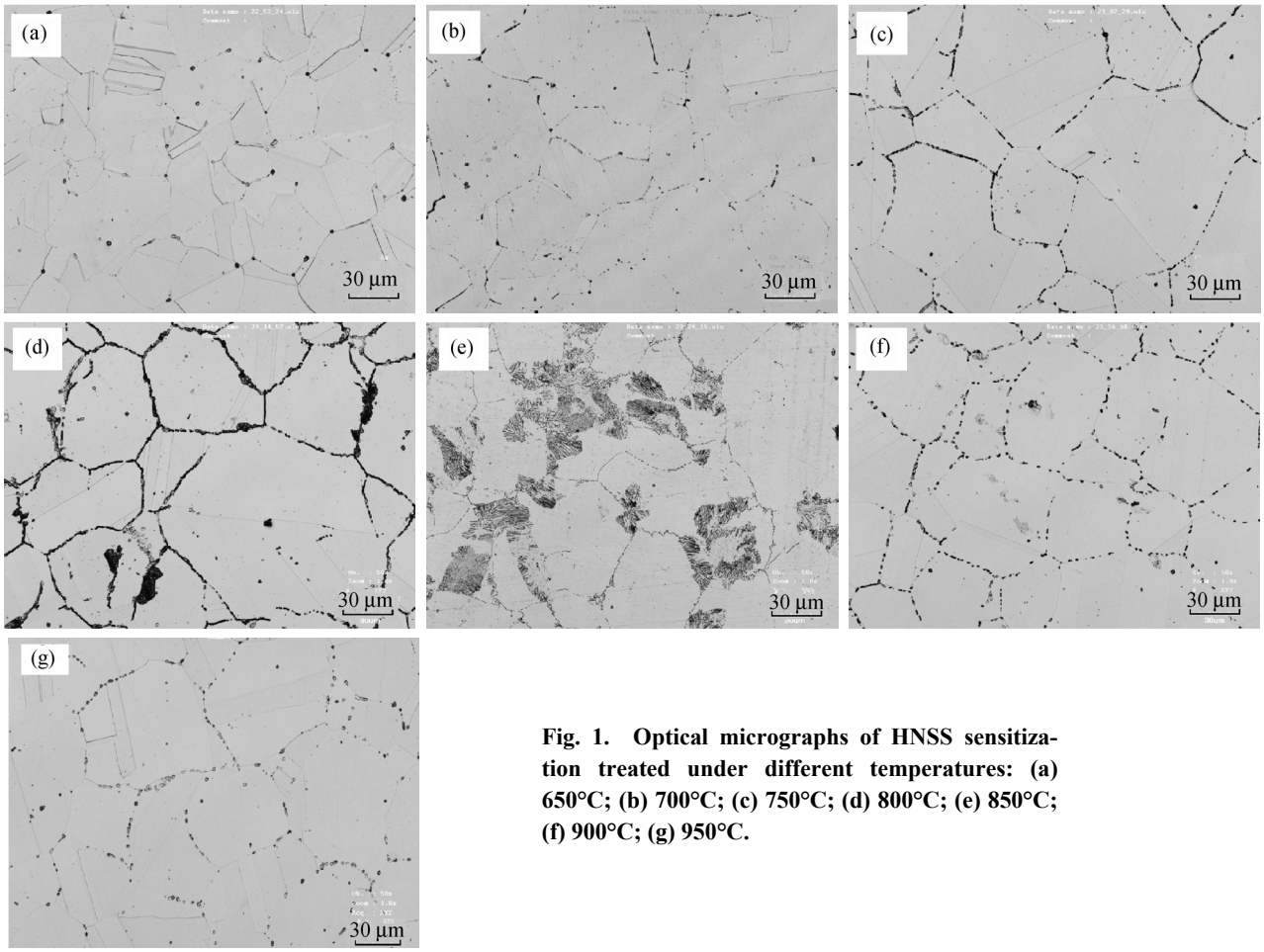

Fig. 1. Optical micrographs of HNSS sensitization treated under different temperatures: (a) 650°C; (b) 700°C; (c) 750°C; (d) 800°C; (e) 850°C; (f) 900°C; (g) 950°C.

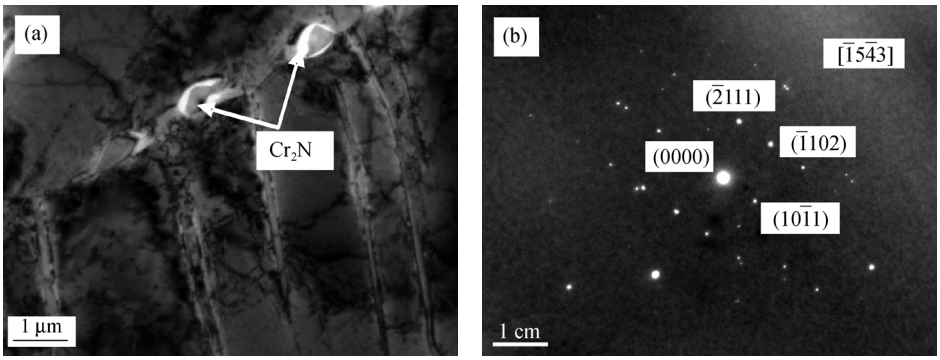

Fig. 2. TEM micrographs of intergranular Cr_2N sensitization treated at 800°C for 2 h: (a) bright field images; (b) SAD pattern.

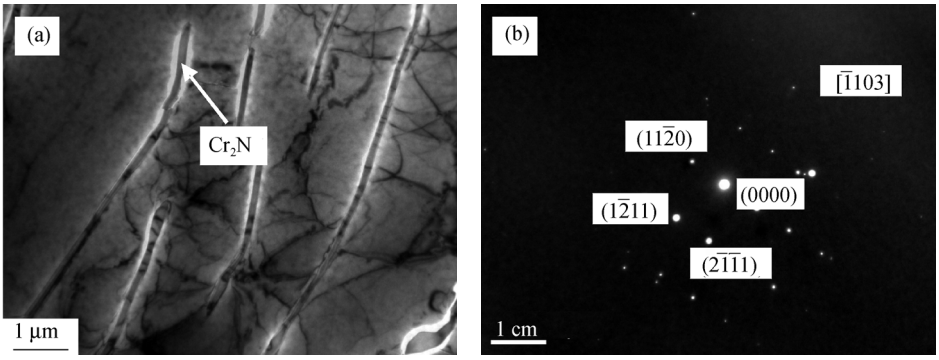

Fig. 3. TEM micrographs of cellular Cr_2N sensitization treated at 850°C for 2 h: (a) bright field images; (b) SAD pattern.

The electrolyte of 0.5 mol/L H_2SO_4+0.01 mol/L KSCN was first attempted to determine the IGC susceptibility of HNSS at 1.667 mV/s scan rate in the present work. The DL-EPR result of the specimen sensitization treated at 850°C shows that no reactivation phenomenon takes place as shown in Fig. 5(a),

and the I_r/I_a and Q_r/Q_a values are equal to zero as shown in Table 2. Increasing the concentration of sulfuric acid to 2 mol/L, the activation peak is higher and no reactivation peak appears as shown in Fig. 5(b). The IGC attack at the surface is not observed in the above experiments. The results indicate that the effect of sulphuric acid on the reactivation is insignificant, and the electrolytes of 0.5 mol/L H_2SO_4+0.01 mol/L KSCN and 2 mol/L H_2SO_4+0.01 mol/L KSCN are not sensitive to chromium-depleted zones and not suitable to examine the IGC of HNSS.

Some researchers [20-21] suggested that the addition of NaCl or hydrochloric acid (HCl) into electrolytes as depassivators which results in the cracking of a passive film in chromium-depleted zones during the reactivation scan, can quantitatively evaluate well the susceptibility to IGC of some stainless steels and super alloys. So the 2 mol/L H_2SO_4+0.01 mol/L KSCN electrolyte was adjusted with the addition of 0.5 mol/L NaCl to check the IGC of the specimen sensitization treated at 650°C with 1.667 mV/s scan rate. But no reactivation peak appears, and the IGC attack was not found at the surface of the specimen. It was believed that the depassivator concentration of NaCl was not enough to breakdown the passive film. When the concentration of NaCl increases to 1 mol/L, the lower reactivation peak can be obtained as shown in Fig. 6, and the IGC attack takes place in the grain boundary. Because the lowest degree of chromium depletion due to the least amount precipitation at 650 °C can be detected, the susceptibility to IGC of the steels sensitization treated at 650-950°C can be examined using the 2 mol/L H_2SO_4+1 mol/L NaCl +0.01 mol/L KSCN electrolyte at 1.667 mV/s. It is confirmed by the latter experiments results.

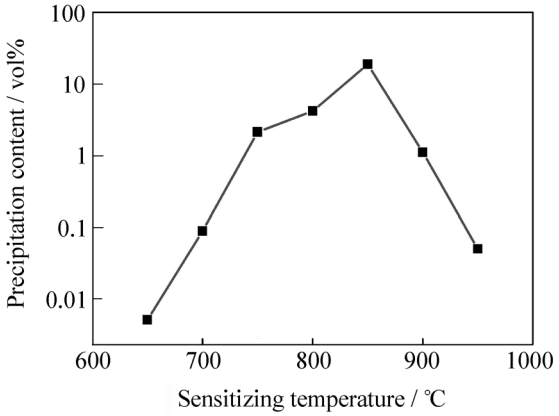

Fig. 4. Relation between the volume fraction of precipitation and sensitizing temperature for 2 h sensitization.

Table 2. Experimental conditions to evaluate IGC susceptibility by the DL-EPR method

Sensitizing temperature / °C	Experimental conditions of DL-EPR test		Evaluation criterion of IGC sensitization		
	Composition of the electrolyte / (mol·L^{-1})	Potential scan rate / (mV·s^{-1})	I_r/I_a	Q_r/Q_a	Etching structure
850	0.5 H_2SO_4+0.01 KSCN	1.667	0	0	no IGC
850	2 H_2SO_4+0.01 KSCN	1.667	0	0	no IGC
650	2 H_2SO_4+0.5 NaCl+0.01 KSCN	1.667	0	0	no IGC
650	2 H_2SO_4+1 NaCl+0.01 KSCN	1.667	0.051	0.047	IGC
650	2 H_2SO_4+1 NaCl+0.01 KSCN	2.5	0	0	no IGC
850	2 H_2SO_4+1 NaCl+0.01 KSCN	0.8333	0.696	1.039	IGC and general corrosion
850	2 H_2SO_4+1 NaCl+0.01 KSCN	1.667	0.485	0.563	IGC
850	2 H_2SO_4+1 NaCl+0.01 KSCN	2.5	0.387	0.461	IGC

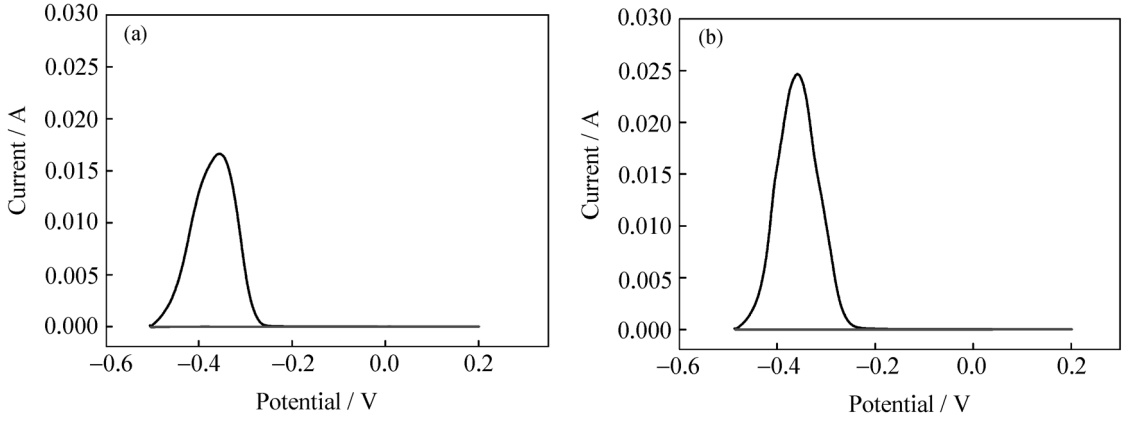

Fig. 5. DL-EPR curves of HNSS sensitization treated at 850°C with different concentrations of sulfuric acid: (a) 0.5 mol/L; (b) 2 mol/L.

The DL-EPR experiments of HNSS sensitizing treated at 850°C were performed in the 2 mol/L

H_2SO_4+1 mol/L NaCl+0.01 mol/L KSCN electrolyte at different scan rates. When increasing the scan rate, the effect of scan rate on I_a is not notable, and its effects on I_r, Q_r, I_r/I_a and Q_r/Q_a are very pronounced as shown in Table 3. The I_r/I_a and Q_r/Q_a values decrease with increasing scan rate. When the DL-EPR experiment is carried out at 0.8333 mV/s, the reactivation behavior is remarkable and the specimen is attacked seriously by IGC and general corrosion as shown in Table 2. The results indicate that the lower scan rate exhibits an obvious effect on the breakdown of the passive film. When the DL-EPR experiment of HNSS sensitization treated at 650°C is carried out at 2.5 mV/s, and other factors being constant, the reactivation peak disappears and the I_r/I_a and Q_r/Q_a values are equal to zero as shown in Fig. 6 and Table 2, respectively. So the 1.667 mV/s scan rate is suitable to evaluate the susceptibility to IGC in 2 mol/L H_2SO_4+1 mol/L NaCl + 0.01 mol/L KSCN electrolyte of HNSS sensitization treated at 650-950°C.

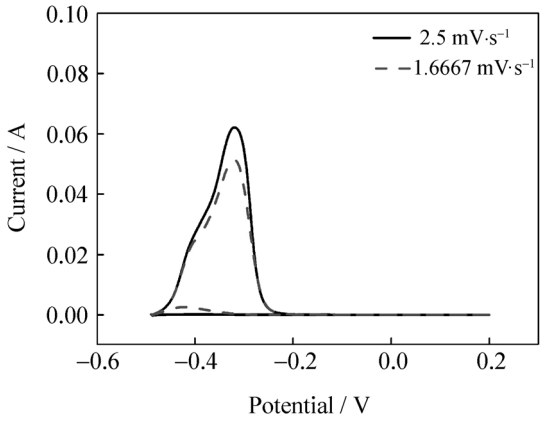

Fig. 6. DL-EPR curves of HNSS sensitization treatment at 650°C at scan rates of 2.5 and 1.667 mV/s.

Table 3. DL-EPR results of HNSS sensitization treated at 850°C

Scan rate / (mV·s^{-1})	I_a / mA	I_r / mA	Q_a / C	Q_r / C	I_r/I_a	Q_r/Q_a
0.8333	85.60	59.55	9.812	10.19	0.6957	1.0385
1.667	88.58	42.92	5.019	2.824	0.4845	0.5627
2.5	80.66	31.2	3.439	1.585	0.3868	0.4609

(2) Influence of sensitizing temperature

The DL-EPR experiments of HNSS sensitization treated at different temperatures in the 2 mol/L H_2SO_4 +1 mol/L NaCl+0.01 mol/L KSCN electrolyte at 1.667 mV/s were done to investigate the effect of sensitizing temperature on the susceptibility to IGC. The influences of sensitizing temperature on I_r, Q_a, Q_r, I_r/I_a and Q_r/Q_a are very obvious as shown in Table 4. The same tendency can be observed that the values of I_r, Q_a, Q_r, I_r/I_a and Q_r/Q_a increase and then decrease with increasing sensitizing temperature. The I_r, I_r/I_a and Q_r/Q_a arrive at the maximum values for the specimen sensitized at 850°C, which indicates that passive film breakdown occurs seriously at this reactivation scan.

Table 4. DL-EPR results of HNSS sensitization treated with different sensitizing temperatures

Sensitization temperature / °C	I_a / mA	I_r / mA	Q_a / C	Q_r / C	I_r/I_a	Q_r/Q_a
650	51.40	2.61	3.416	0.159	0.0508	0.0466
700	59.50	4.64	3.860	0.349	0.0780	0.0904
750	54.70	15.90	3.959	1.432	0.2907	0.4058
800	76.35	31.16	4.549	2.186	0.4081	0.4855
850	88.58	42.92	5.019	2.824	0.4845	0.5627
900	60.40	6.40	3.730	0.400	0.1060	0.1070
950	49.40	3.57	3.258	0.200	0.0723	0.0614

Fig. 7 is the optical micrographs of HNSS sensitization treated under different temperatures after DL-EPR experiments. When the specimen is sensitization treated at 650°C, only a few dot-like cavities can be found along some grain boundaries as shown in Fig. 7(a). Increasing the sensitizing temperature to 700°C, some dot-like cavities and discontinuous ditches appear along grain boundaries (Fig. 7(b)). The more discontinuous and some continuous ditches are observed along grain boundaries when the specimen is sensitization treated at 750°C (Fig. 7(c)). The more continuous ditches appear in the boundaries, and the ditches become deeper and wider at 800°C (Fig. 7(d)). The specimen sensitization treated at 850°C suffered serious attack along the grain boundaries and inside the grain as shown in Fig. 7(e). When increasing the temperature from 900 to 950°C, some discontinuous deeper ditches and some dot-like cavities appear along the grain boundaries as shown in Figs. 7(f) and 7(g), respectively. The results show that the degree of IGC attack increases and then decreases with increasing sensitizing temperature, which is in well agreement

with the change tendency of I_r/I_a and Q_r/Q_a.

It is well-known that the IGC of stainless steels is closely related to the depletion of chromium along the grain boundaries. The susceptibility to IGC is usually caused by the precipitation of Cr carbides or other chromium-rich phases along the boundaries. The carbon content of stainless steel is believed to play a key role in the precipitation of Cr carbides. But in the present work, no any precipitation of Cr carbides was detected by TEM analysis, and only the chromium-rich phase Cr_2N was found along grain boundaries and inside gains. The precipitation of chromium carbides is possible to be suppressed or be very little due to a lower carbon content of 0.022wt% and a high nitrogen content of 0.88wt% in HNSS. So it was suggested that chromium depletion in HNSS was attributed to the precipitation of Cr_2N, which resulted in the susceptibility to IGC. The precipitation amount of Cr_2N should take charge of the degree of IGC attack for HNSS. When HNSS was sensitization treated at 850°C, lots of cellular Cr_2N precipitation along grain boundaries and inside grains could be observed, which resulted in serious chromium depletion along grain boundaries and in some area inside grains, and HNSS suffered the most serious attack of IGC. The change tendency of precipitation amount was consistent with that of DL-EPR results and the micrographs of HNSS attacked by IGC. So the susceptibility to IGC of HNSS sensitization treated at 650-950°C could be evaluated well in the 2 mol/L H_2SO_4+1 mol/L NaCl+ 0.01 mol/L KSCN electrolyte at a scan rate of 1.667 mV/s.

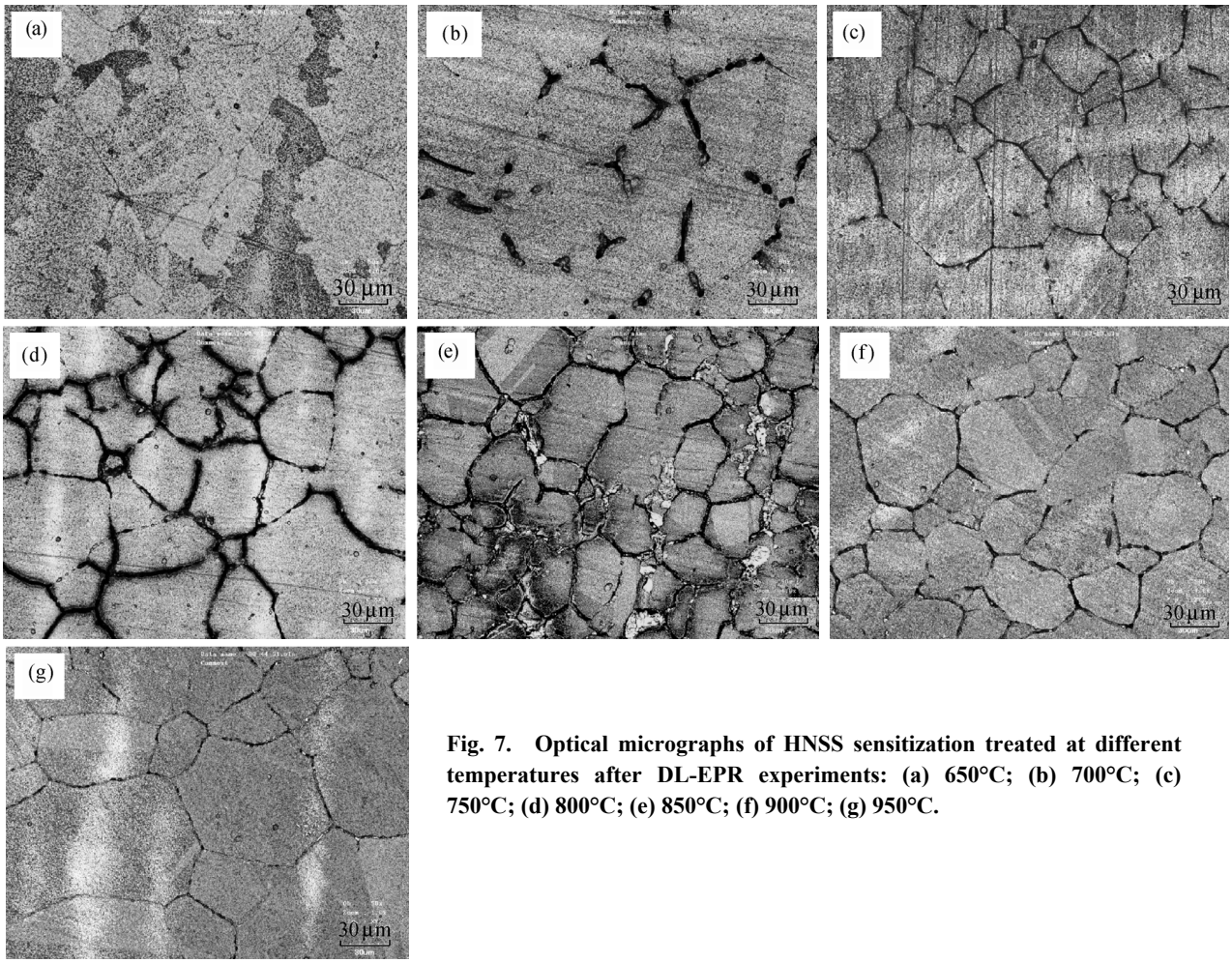

Fig. 7. Optical micrographs of HNSS sensitization treated at different temperatures after DL-EPR experiments: (a) 650°C; (b) 700°C; (c) 750°C; (d) 800°C; (e) 850°C; (f) 900°C; (g) 950°C.

Wu [16] presented that HNSS with Mo addition showed a better resistance to IGC in comparison with HNSS without any addition of Mo, which was attributed to the synergistic effect of Mo and N. In our previous work [22], the sensitization treated 18Cr-18Mn-0.9N high nitrogen austenitic stainless steels exhibited the susceptibility to IGC in 0.5 mol/L H_2SO_4+0.01 mol/L KSCN at 30°C and 1.667 mV/s scan rate. But in the present research, the solution was not sensitive to the chromium depletion zones of HNSS with the addition of 2.26wt% Mo, so 2 mol/L NaCl as depassivators was added into the solution to increase its sensitivity. The result indicated that the addition of Mo in HNSS stabilizes the passive film to prevent the attack of IGC during the reactivation scan, and the synergistic effect of Mo and N was also possi-

ble to play an important role in present IGC process of HNSS.

4. Conclusions

(1) The precipitation is mainly composed of Cr_2N phases at the sensitizing temperature range. The volume fraction of precipitation increases then reduce with increasing sensitizing temperature. The change tendency is consistent with the DL-EPR results and micrographs of HNSS attacked by IGC.

(2) The effect of sulphuric acid on the reactivation is insignificant. The addition of NaCl as depassivators is an effective way to improve the formation of the cracking of a passive film in chromium-depleted zones during the reactivation scan. With decreasing scan rate, the values of I_r/I_a and Q_r/Q_a increase. The scan rate exhibits an obvious effect on the breakdown of the passive film. The 2 mol/L H_2SO_4+1 mol/L NaCl+0.01 mol/L KSCN solution is suitable to check the susceptibility to IGC of HNSS at the sensitizing temperature ranging from 650 to 950°C at a suitable scan rate of 1.667 mV/s in the present work.

(3) Chromium depletion in HNSS is attributed to the precipitation of Cr_2N, which results in the susceptibility to IGC. The synergistic effect of Mo and N is suggested to play an important role in stabilizing the passive film to prevent the attack of IGC.

References

[1] U.K. Mudali, C.B. Rao, and B. Raj, Intergranular corrosion damage evaluation through laser scattering technique, *Corros. Sci.*, 48(2006), No.4, p.783.

[2] P. Muraleedharan, J.B. Gnanamoorthy, and P. Rodriguez, Degree of sensitization and intergranular stress corrosion cracking susceptibility of type 304 stainless steel, *Corrosion*, 52(1996), No.10, p.790.

[3] Z. Stonawska, M. Svoboda, M. Sozanska, *et al.*, Structural analysis and intergranular corrosion tests of AISI 316L steel, *J. Microsc.*, 224(2006), No.1, p.62.

[4] M. Terada, M. Saiki, I. Costa, *et al.*, Microstructure and intergranular corrosion of the austenitic stainless steel 1.4970, *J. Nucl. Mater.*, 358(2006), No.1, p.40.

[5] U.K. Mudali, R.K. Dayal, J.B. Gnanamoorthy, *et al*., Relationship between pitting and intergranular corrosion of nitrogen-bearing austenitic stainless steels, *ISIJ Int.*, 36(1996), No.7, p.799.

[6] M. Terada, D.M. Escriba, and I. Costa, *et al.*, Investigation on the intergranular corrosion resistance of the AISI 316L(N) stainless steel after long time creep testing at 600°C, *Mater. Charact.*, 59(2008), No.6, p.663.

[7] A.F. Padilha and P.R. Rios. Decomposition of austenite in austenitic stainless steels, *ISIJ Int.*, 42(2002), No.4, p.325.

[8] P. Novak, R. Stefec, and F. Franz, Testing the susceptibility of stainless steel to intergranular corrosion by a reactivation method, *Corrosion*, 31(1975), No.10, p.344.

[9] R.F.A. Jargelius, S. Hertzman, E. Symniotis, *et al.*, Evaluation of the EPR technique for measuring sensitization in type 304 stainless steel, *Corrosion*, 47(1991), No.6, p.429.

[10] A.P. Majidi and M.A. Streicher, Potentiodynamic reactivation method for detecting sensitization in AISI 304 stainless steels, *Corrosion*, 40(1984), No.11, p.584.

[11] M. Matula, L. Hyspecka, M. Svoboda, *et al.*, Intergranular corrosion of AISI 316L steel, *Mater. Charact*., 46(2001), No.2-3, p.203.

[12] M.K. Ahn, H.J. Kwon, and J.H. Lee, Predicting susceptibility of alloy 600 to intergranular stress corrosion cracking using a modified electrochemical potentiodynamic reactivation test, *Corrosion*, 51(1995), No.6, p.441.

[13] A. Pardo, M.C. Merino, A.E. Coy, *et al.*, Influence of Ti, C and N concentration on the intergranular corrosion behaviour of AISI 316Ti and 321 stainless steels, *Acta Mater.*, 55(2007), No.7, p.2239.

[14] T. Amadou, C. Braham, and H. Sidhom, Double loop electrochemical potentiodynamic reactivation test optimization in checking of duplex stainless steel intergranular corrosion, *Metall. Mater. Trans. A*, 35(2004), No.11, p.3499.

[15] G.H. Aydogdu and M.K. Aydinol, Determination of susceptibility to intergranular corrosion and electrochemical reactivation behavior of AISI 316L type stainless steel, *Corros. Sci.*, 48(2006), No.11, p.3565.

[16] X.Q. Wu, S. Xu, J.B. Huang, *et al.*, Uniform corrosion and intergranular corrosion behavior of nickel-free and manganese alloyed high nitrogen stainless steels, *Mater. Corros.*, 59(2008), No.8, p.676.

[17] T.F. Wu, T.P. Cheng, and W.T. Tsai, Effect of electrolyte composition on the electrochemical potentiodynamic reactivation behavior of Alloy 600, *J. Nucl. Mater.*, 295(2001), No.2-3, p.233.

[18] H.B. Li, Z.H Jiang, M.H. Shen, *et al.*, Manufacturing high nitrogen austenitic stainless steels by nitrogen gas alloying and adding nitrided ferroalloys, *J. Iron. Steel. Res. Int.*, 14(2007), No.3, p.63.

[19] T.H. Lee, S.J. Kim, and S. Takaki, Time-temperature-precipitation characteristics of high-nitrogen austenitic Fe-18Cr-18Mn-2Mo-0.9N steel, *Metall. Mater. Trans. A*, 37(2006), No.12, p.3445.

[20] N. Lopez, M. Cid, M. Puiggali, *et al.*, Application of double loop electrochemical potentiodynamic reactivation test to austenitic and duplex stainless steels, *Mater. Sci. Eng. A*, 229(1997), No.1-2, p.123.

[21] Y. Cetre, P. Eichner, G. Sibaud, *et al.*, Corrosion in chemical and parachemical industries, [in] *Proceedings of the 3rd European Conference on Corrosion*, Lyon, 1997, p.C4.1.

[22] H.B. Li, *Metallurgical Fundamental and Properties of High Nitrogen Austenitic Stainless Steels* [Dissertation] (in Chinese), Northeastern University, Shenyang, 2008, p.113.